"Crowned" Fe_4S_4 Clusters as Electrochemical Metal Ion Sensors

Robertus J. M. Klein Gebbink,[a] Stephen I. Klink,[a] Martinus C. Feiters,*[a] and Roeland J. M. Nolte*[a]

Keywords: Iron-sulfur clusters / Crown ethers / Electrochemical devices / Host-guest chemistry

A series of Fe_4S_4 cluster compounds, **I**, **III**, and **V**, in which the cuboidal cluster core is appended with four crown ether thiolate ligands, and **II** and **IV**, bearing thiolate ligands without crown ether parts, has been synthesized and characterized. The spectroscopic and electrochemical properties of these compounds are determined by the electronic nature of the thiolate ligands. Only in the case of **III**, where a very short α-thioacetyl linker was used to connect the crown ether ligands to the cluster core, was a restricted conformational freedom of the ligand observed. A detailed electrochemical study of the influence of alkali and earth alkali metal ions (Li^+, Na^+, K^+, Mg^{2+}, and Ba^{2+}) on the reversible $2^-/3^-$ reduction of the cluster compounds was performed. In the case of the crown ether appended clusters **I**, **III**, and **V**, the addition of these metal ions resulted in an anodic shift, i.e. in positive direction, of the reduction potential (modulation effect) and to larger current responses (promotion effect). The magnitude of the modulation effects is determined by the binding affinity of the metal ions in the crown ether ligands, and by the distance between bound metal ions and the redox active cluster core. Variation of the linker between the cluster core and the metal ion binding site resulted in cluster compounds with almost inverse selectivities for e.g. K^+ and Ba^{2+} in the case of **I** and **III**. For the large effects found for compound **I** a lariat binding mode is proposed.

Introduction

Iron sulfur clusters play various roles as prosthetic groups in proteins. Their main function is to catalyze electron transfer reactions, e.g. to another redox active prosthetic group within a protein, or from one protein to another.[1] In a biological environment, tetranuclear Fe_4S_4 clusters generally exist in oxidation states that are designated as $3^-/2^-/1^-$ when the charges on the cysteinyl ligands are considered together with the core charge.[2] Synthetic thiolate clusters of this type show a somewhat richer redox chemistry; they can exist in four distinct oxidation states, $4^-/3^-/2^-$ and 1^-.[3] Early studies on biological and synthetic systems have shown that the potentials at which these states interconvert are strongly influenced by the environment of the cluster. Factors such as hydrogen bonding to the cluster, electron-donating or -accepting properties of the thiolate ligands, hydrophobicity of the ligands, and solvent polarity are all important in determining the actual values of the redox potentials.[4] In general, it can be said that the (partial) electron delocalization in the clusters is the reason why these systems are easily influenced by polarizing forces.

One of the challenges in the field of electrochemical sensory devices is to develop molecular systems that selectively recognize metal ions in general, and alkali and alkaline earth metal ions in particular.[5] Many of these systems are based on transition metal complexes, because they have a rich and well-understood electrochemistry. In these systems a binding site for the above-mentioned metal ions is located closely to a transition metal ion. Upon binding of a metal ion the redox potential of the transition metal complex is changed. This can be caused either by through-space electrostatic interactions or communication via various bond linkages between the binding site and the redox-active center. In the latter case the connector between the binding site and the redox-active site should be conducting in order to achieve the desired effect, whereas in the former case this is not required. In either case, the transition metal ion should be easily polarized to undergo a change in its redox potential. Two examples of such polarizable systems are ferrocene and $[Ru(bipy)_3]^{2+}$, which have both been frequently used in electrochemical devices.[5]

Fe_4S_4 thiolate clusters can also be considered as suitable building blocks for this purpose, as (i) they have a rich and well-defined electrochemistry, (ii) their redox potentials are highly sensitive to polarizing effects, (iii) they can be relatively easily functionalized, and (iv) four ligands can be used to influence one redox center. For these reasons, we decided to study thiolate clusters as the redox-active site for the recognition of alkali and alkaline earth metal ions. As mentioned earlier, these clusters bear a 2− or 3− overall negative charge in their most stable forms, whereas most other systems used for this purpose are neutral or positively charged. These clusters are therefore expected to lack repulsive Coulomb forces that disturb the interaction with metal ions; instead, one can take advantage of attractive Coulomb forces to favour it.

In this paper, the synthesis, characterization, and properties as electrochemical devices of a small series of crown ether substituted clusters will be presented. A simple aza crown ether compound, 1-aza-4,7,10,13,16-pentaoxacyclooctadecane (monoaza-18-crown-6), was used as the metal ion binding unit because of its ease of functionalization,

[a] Department of Organic Chemistry, NSR Center, University of Nijmegen, Toernooiveld, NL-6525 ED Nijmegen, The Netherlands
Fax: (internat.) + 31-24/365-2676
E-mail: mcf@sci.kun.nl

  1434−1948/00/0202−253 $ 17.50+.50/0

and its well-documented binding properties towards metal ions.[6] The binding selectivity of this crown ether is mainly determined by its size compatibility with a metal ion guest, and increases in the order $Li^+ \approx Mg^{2+} < Na^+ < K^+ \approx Ba^{2+}$.

First of all, three cluster compounds **I**, **III**, and **V** were synthesized with different crown ether thiol ligands. The actual binding unit is not changed in this small series, but the spacer units and the nature of the thiol groups are. In addition, two cluster compounds **II** and **IV** were synthesized and to some extent studied, as these cluster compounds lack the crown ether moieties and can therefore be considered as model compounds.

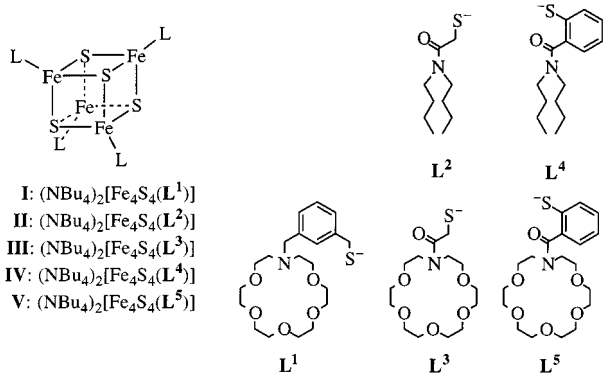

Results and Discussion

Ligand Synthesis

The synthesis of ligand $\mathbf{L^1}$H is depicted in Scheme 1. Starting from α,α′-dibromo-*m*-xylene, one of the bromide substituents was replaced by a thioacetyl group using a procedure described by Kellogg and co-workers[7] in which freshly distilled thioacetic acid was treated with K_2CO_3 to obtain the thioacetate nucleophile. After purification, the desired monobromide **1** was coupled to monoaza-18-crown-6 in DMF in the presence of base. The final step involved the hydrolysis of the thioacetyl function to the desired thiol. This reaction proceeded smoothly under acidic conditions in methanol (3% HCl) and under an inert gas.[8] Due to the presence of an internal base, i.e. the tertiary amine group, $\mathbf{L^1}$H is prone to dimerize under aerobic conditions. This compound was, therefore, kept strictly under N_2 during workup and storage. The overall yield of $\mathbf{L^1}$H was 41%.

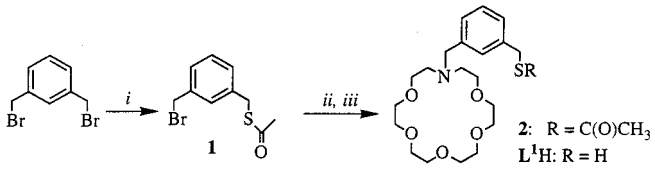

Scheme 1. Synthesis of ligand $\mathbf{L^1}$H: (*i*) K_2CO_3, $CH_3C(O)SH$, DMF; (*ii*) monoaza-18-crown-6, K_2CO_3, DMF; (*iii*) 3% HCl/MeOH

In the synthesis of ligand $\mathbf{L^2}$H and $\mathbf{L^3}$H, the spacer unit was added to the respective secondary amines, di-*n*-butylamine and monoaza-18-crown-6, prior to introduction of the protected thiol functionality, as is shown in Scheme 2. The respective secondary amines were acylated at the nitrogen position by treatment with freshly distilled α-chloroacetyl chloride, followed by substitution of the halide by a thioacetyl group as discussed above. The desired thiols were then isolated after hydrolytic deprotection of the thioacetate by treatment with 3% HCl in methanol. Overall yields were 16 and 52% for $\mathbf{L^2}$H and $\mathbf{L^3}$H, respectively. Because these compounds lack an internal base, they are less sensitive to oxidative dimerization than $\mathbf{L^1}$H.

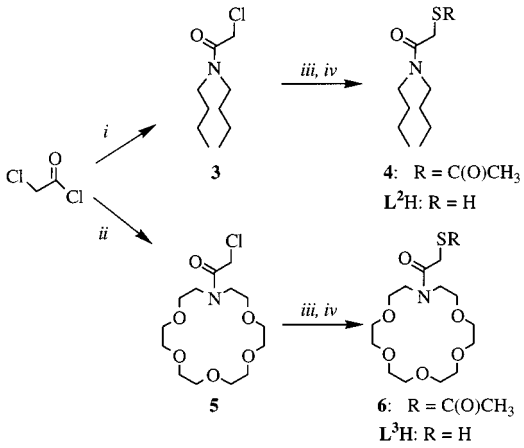

Scheme 2. Synthesis of ligands $\mathbf{L^2}$H and $\mathbf{L^3}$H: (*i*) di-*n*-butylamine, K_2CO_3, DMF; (*ii*) monoaza-18-crown-6, K_2CO_3, toluene; (*iii*) K_2CO_3, $CH_3C(O)SH$, DMF; (*iv*) 3% HCl/MeOH

A different strategy was used for the synthesis of $\mathbf{L^4}$H and $\mathbf{L^5}$H (Scheme 3). In the first step, 2-thiosalicylic acid was protected as its disulfide, which was then converted into the corresponding diacid chloride by treatment with thionyl chloride. Acylation of secondary amines with this diacid chloride proceeded smoothly in the presence of triethylamine as a base. The final step, cleavage of the disulfide bond to yield two identical thiols, was performed in a water/dioxane mixture with triphenylphosphane as the nucleophile, under acidic conditions.[9] Pure samples of $\mathbf{L^4}$H and $\mathbf{L^5}$H could be obtained by column chromatography. The overall yields were 48 and 52% for $\mathbf{L^4}$H and $\mathbf{L^5}$H, respectively.

Synthesis and Characterization of Substituted Fe_4S_4 Clusters

Cluster compounds **I**−**V** were synthesized by ligand exchange reactions (Scheme 4),[10] and were isolated as dianionic species with either tetraalkylammonium or tetraphenylphosphonium counter ions. In one approach, these exchange reactions are based on an acid-base equilibrium, in which a more acidic thiol replaces a more basic thiolate ligand from an $Fe_4S_4(SR)_4$ cluster.[11] By making use of volatile thiols as the leaving group, e.g. tertiary butyl thiol, the equilibrium is easily driven to one desired product by

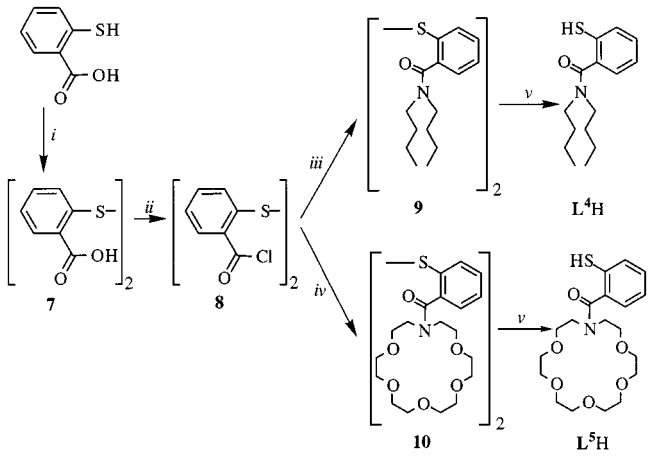

Scheme 3. Synthesis of ligands $\mathbf{L^4}$H and $\mathbf{L^5}$H: (*i*) H_2O_2, KOH, water; (*ii*) $SOCl_2$; (*iii*) di-*n*-butylamine, TEA, CH_2Cl_2; (*iv*) monoaza-18-crown-6, TEA, CH_2Cl_2; (*v*) PPh_3, dioxane/water/HCl

applying a "dynamic" vacuum. The other approach makes use of an Fe_4S_4 cluster that bears good leaving groups such as Cl^- ligands. The thiol used in these reactions is first deprotonated in order to make it a better nucleophile and to prevent the formation of HCl. Both methods were applied in the syntheses of clusters **I**−**V** since each of them has its advantages. The first method proceeds under very mild conditions without the need of any additive, whereas the second method is much faster but suffers from the fact that a base has to be added which may lead to counter ion scrambling.

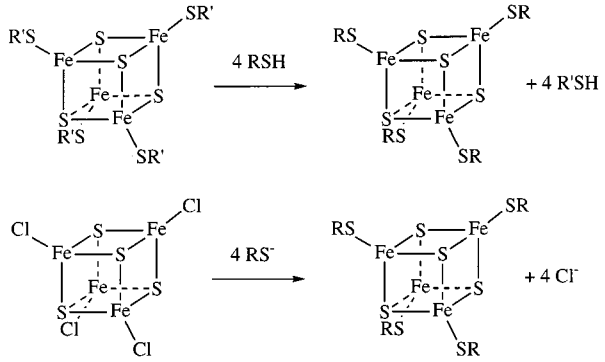

Scheme 4. Preparation of Fe_4S_4 cluster compounds by ligand exchange reactions

Prior to the synthesis of the cluster compounds, test reactions were performed in situ in an electrochemical cell, and followed by differential pulse voltammetry (DPV). With this procedure, the quality of the freshly prepared thiols was tested, and an indication of the electrochemical characteristics of the final cluster compounds was obtained. On a preparative scale, the desired cluster compounds **I**−**V** were isolated as black oils after filtration of the crude reaction mixtures, followed by repeated precipitations from solution, and in vacuo removal of residual solvent.

Initial spectroscopic characterization of the isolated cluster compounds was performed by means of UV/Vis spectroscopy. Their UV/Vis characteristics closely matched the properties of related cluster compounds[12][13] and confirmed the integrity of the cubane core in these newly synthesized compounds (see Experimental Section). Further characterization was performed by NMR spectroscopy and electrochemical techniques (vide infra). NMR showed that all isolated cluster compounds contained residual solvent. In spite of the above workup procedures, and after several crystallization attempts and washings of the isolated products with various nonsolvents, it was not possible to remove these solvent traces. Elemental analyses of the isolated cluster compounds were therefore not performed.

NMR spectra of Fe_4S_4 cluster compounds in general are characterized by large chemical shifts of nuclei close to the cluster core and by broadened signals, due to the thermal accessibility of paramagnetic excited states at ambient temperature.[14] These two features can be observed in Figure 1, which shows the ^{1}H-NMR spectrum of cluster **III** in [D_7]DMF solution. In Table 1, the isotropic shifts are listed for the protons closest to the cluster core in clusters **I**−**V**. These shifts are defined as the difference in chemical shift for a given nucleus in the free ligand and in the cluster compound. For clusters **I**−**III** the shifts all have a negative sign, whereas for clusters **IV** and **V** some have a positive sign. The latter observation is a characteristic feature of aryl thiolate-substituted clusters and is correlated to the sign of spin density at the respective carbon atom in the aromatic ring. For aliphatic ligands, the sign has been shown to be non-alternative; its magnitude depends strongly on the distance between the metal center and the hydrogen nucleus.[14]

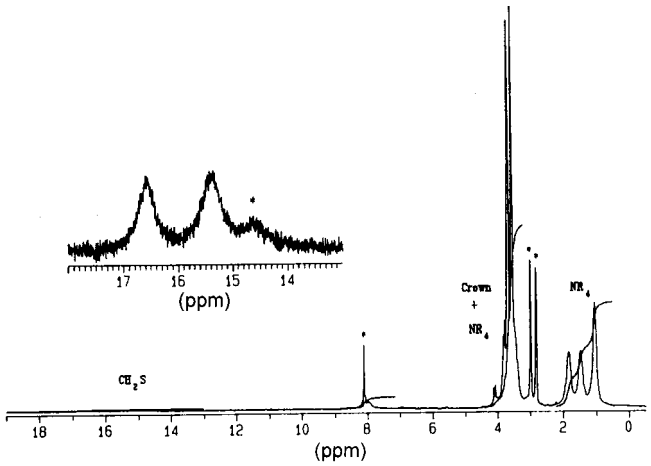

Figure 1. ^{1}H-NMR spectrum of cluster compound **III** in [D_7]DMF (the asterisks denote unassigned peaks and residual solvent peaks)

These general features were also found in temperature-dependent NMR studies on clusters **III** and **IV**, in the temperature range 298−350 K. The experiments showed that the isotropic shifts for these cluster compounds changed in magnitude upon increase of the temperature, due to a higher occupation of the first excited state, whereas their sign did not change. The temperature dependencies of the isotropic shifts are listed in Table 1, and were analyzed as linear relationships. Similar linear dependencies have been

Table 1. Isotropic shifts of ligand protons in cluster compounds **I**−**V**, together with their temperature dependence (temperature range: 300−340 K; solvent: [D_7]DMF or [D_6]DMSO, see Experimental Section)

Compound		Ligand δ [ppm]	Cluster δ [ppm]	ΔH_{iso} [ppm]	$\Delta H_{iso}/T$ [Hz/K]
I	CH_2S	3.62	15.08	−11.46	n.d.[a]
II	CH_2S	3.36	13.83	−10.47	n.d.[a]
III	CH_2S	3.76	15.35	−11.59	−3.32
			16.58	−12.82	−3.32
IV	*p*ArH	7.25	3.73	3.52	0.43
	*o*ArH	″	5.32	1.93	0.31
	*m*ArH	″	7.97	−0.72	−0.20
	*m*ArH	″	8.28	−1.03	−0.27
V	*p*ArH	7.25	n.o.[b]	−	−
	*o*ArH	″	5.29	1.96	n.d.[a]
	*m*ArH	″	7.96	−0.71	n.d.[a]
	*m*ArH	″	8.39	−1.14	n.d.[a]

[a] n.d.: not determined. − [b] n.o.: not observed.

observed for other cluster compounds in the same temperature range.[14][15]

An interesting feature from Figure 1 is the fact that the CH_2−S hydrogen signals in cluster **III** appeared as two singlets with approximately equal intensity. Apparently, the ligands in **III** have a restricted rotational freedom, which results in nonequivalent methylene hydrogen atoms due to the angular dependence of their isotropic shifts. Similar observations have been made for the cysteinyl methylene hydrogenatoms in iron-sulfur proteins and in oligopeptide model compounds.[16][17] For cluster **II**, only one signal was observed for the CH_2−S protons, suggesting that in **III** the crown ethers play a determining role in restricting the conformation of the ligands.

The electrochemical properties of **I**−**V** were studied by means of cyclic voltammetry (CV) and differential pulse voltammetry (DPV) in DMF. This solvent was chosen because both R_4N and Ph_4P salts of iron-sulfur clusters are soluble in it. Numerical data of the study are presented in Table 2.

Table 2. Electrochemical data for the 2−/3− reduction of cluster compounds **I**−**V** in DMF[a]

	CV			DPV	
	$E_{1/2}$ [V][b]	i_b/i_f	ΔE_p	E_p [V][b]	$W_{1/2}$
I	−1.74	0.68	85	−1.74	160
II	−1.65	0.86	221	−1.66	100
III	−1.58	0.80	213	−1.58	150
IV	−1.52	0.56	170	−1.50	140
V	−1.50	0.49	270	−1.48	284

[a] For conditions see Experimental Section. Pt working electrode. − [b] Potentials are given relative to the Fc/Fc^+ redox couple in the same solvent.

The halfwave potentials ($E_{1/2}$) for the 2−/3− reduction of clusters **I**, **IV**, and **V** compare well with values for simple, related thiolate clusters. For $[Fe_4S_4(SCH_2Ph)_4]^{2-}$ and $[Fe_4S_4(SPh)_4]^{2-}$ the $E_{1/2}$ values have been reported to be −1.74 and −1.52 V, respectively.[18] The corresponding $E_{1/2}$ for cluster **II** has an intermediate value; this reflects the fact that the thiolate ligands in this compound have relatively strong electron-accepting properties. The halfwave potentials of these cluster compounds are therefore solely determined by the electronic properties of the thiolate ligands. In contrast, the $E_{1/2}$ value of cluster **III** was found to be 70 mV more positive than that of cluster **II**. This is probably caused by the crown ethers, which are in close proximity of the cluster core due to the short acetyl spacers. The exact nature of the influence of the crown ethers on the reduction potential is not yet understood. NMR experiments showed that the ligands in **III** have restricted conformations (vide supra).

For all cluster compounds, the peak separations (ΔE_p) in the cyclic voltammograms and the peak widths at half peak height ($W_{1/2}$) in the differential pulse voltammograms were larger than the theoretical values of 59 mV and 90.4 mV, respectively. These deviations indicate that the electron-transfer rate between the electrode and the cluster compound is slow on the experimental time scale. A reason for the electrochemically quasi-reversible redox processes, in the case of the crown ether-functionalized compounds, could be the shielding of the cluster core from the electrode. Direct contact between the electrode and the redox-active species is desirable, as diminished contact delays the velocity of electron-transfer between the redox active moiety and the electrode, resulting in large peak separations. In addition, the ratio of the peak currents for the backward and the forward processes (i_b/i_f) in CV did not approach the value of 1 in most cases.

To obtain insight into the factors that govern the electrochemical properties of the above-mentioned cluster compounds, a more elaborate study was undertaken for compounds **IV** and **V**. First of all, scan rate dependent CV experiments were performed. The $E_{1/2}$ values of both clusters were found to be independent of the scan rate, whereas ΔE_p increased considerably with increasing scan rate. A linear relationship was found between the cathodic peak current ($i_{p,c}$) and the square root of the scan rate ($\upsilon^{1/2}$), suggesting that the mass transport of redox-active species toward the Pt electrode was diffusion-controlled. In addition, it was found that at higher scan rates the 2−/3− reduction was chemically more reversible. The 2−/3− reductions can therefore be described as chemically quasi-reversible, which implies that the reduction of the cluster core is followed by a chemical reaction that is fast enough to influence the voltammetric analysis (EC mechanism). This can either be due to the coordinating properties of the solvent, which would lead to diminished stability of the generated 3− cluster, or to ligand reactivity.

For cluster compound **IV**, the solvent and the type of electrode in the electrochemical experiments were varied. In solvents with relatively high ε, the $E_{1/2}$ values of **IV** were similar to those of $[Fe_4S_4(SPh)_4]^{2-}$, i.e. −1.52 V and −1.40 V in DMF and acetonitrile, respectively. In dichloromethane, the $E_{1/2}$ for **IV** was found to be 100 mV more negative than for $[Fe_4S_4(SPh)_4]^{2-}$. This might be the result of ion pair formation or (diminished) interactions of the cluster with the solvent. The electrochemical reversibility was im-

proved in acetonitrile. The best results were obtained, however, when a pyrolytic graphite-edge (PGE) electrode was used. With this electrode, also in DMF, a rather fast electron transfer was observed, together with a somewhat higher chemical reversibility. Compared to Pt electrodes PGE electrodes are chemically less inert, i.e. due to surface oxidation, interactions between electrode and redox-active species are more plausible.

In conclusion, it appears that the relatively large organic ligands influence the electrochemical behaviour of cluster compounds **I**−**V** to some extent. Due to shielding of the negatively charged cluster core by the large organic ligands, which apparently slows down the electron transfer from electrode to cluster core, the observed electrochemical processes were not always ideal. By varying the circumstances under which the compounds were studied, however, it was shown that these clusters inherently undergo reversible redox transitions.

Electrochemical Recognition of Alkali and Alkaline Earth Metal Ions

The effects of alkali and alkaline earth metal ions on the $E_{1/2}$ for the 2−/3− transition of cluster compounds **I**, **III**, **IV**, and **V**, were investigated by performing DPV experiments in the presence of varying amounts of perchlorate salts of lithium, sodium, potassium, magnesium, and barium. The use of the DPV technique has the advantage that very small amounts of material can be used. This technique also has a higher resolution compared to CV. Figure 2 shows the changes in the differential pulse voltammograms of cluster compound **I** and of **V** upon the addition of Ba^{2+} ions. The peak potentials for the reduction of both compounds shift to more positive values, i.e. the clusters are more easily reduced to the 3− form. Compound **I** exhibited so-called multi-wave behaviour, whereas **V** showed a continuous shift of its E_p (vide infra). Similar titrations were performed with the cluster compounds **III** and **IV**.

In all cases, a change in E_p occurs in an anodic, i.e. in a positive direction (Table 3). The magnitude of this change depends on the cluster compounds as well as on the metal ions. For example, Ba^{2+} ions give a shift in E_p of 190 mV with **I**, but only 20 mV with **IV**. The crown ether parts in the ligands thus appear to be essential to give large changes in the electrochemical properties of the Fe_4S_4 core upon addition of metal ions. A more detailed investigation of the effect of the crown ether ligands on the electrochemical behaviour toward alkali and alkaline earth metal ions was performed with compounds **I**, **IV**, and **V**, and is described below.

Table 3. Changes in E_p for the reduction of compounds **I**, **III**, **IV**, and **V** upon addition of 10 equivalents of metal ion[a]

	I	III	IV	V
Li^+	90 (120)	(0)	0 (0)	0 (10)
Na^+	30 (n.d.)[b]	–	0 (10)	50 (60)
K^+	40[c] (n.d.)[b]	–	0 (10)	50 (60)
Mg^{2+}	190[d] (290)[e]	(130)	30 (90)	70 (110)
Ba^{2+}	190[d] (210)	(120)	20 (50)	30 (50)

[a] In parentheses the E_p change when a large excess (100 equivalents) of metal ion is added. − [b] n.d. = not determined. − [c] Reached after 2 equivalents had been added. − [d] Reached after 4 equivalents had been added. − [e] Small additional peak observed.

Promotion and Modulation Effects

First of all, it is worthwhile to explain the difference between promotion and modulation effects on the electrochemical properties of redox active species. In general, promotion effects involve an improvement of both current response and electrochemical reversibility of a redox process, and in addition often involve an increase of peak currents after repetitive CV scans. Modulation effects involve changes in the potential of a redox process. The electrochemistry of large biomolecules often suffers from very poor current responses due to slow electron transfer from the redox active entity, embedded in the protein core, to the electrode.[19] Addition of a promoter increases the electron-transfer rate either by improving the protein-electrode interaction or by mediating electron transfer. Generally, promoters are polar or charged compounds that bear coordinating groups. Sometimes the use of a promoter also results in an altered $E_{1/2}$. In that case this compound behaves as a

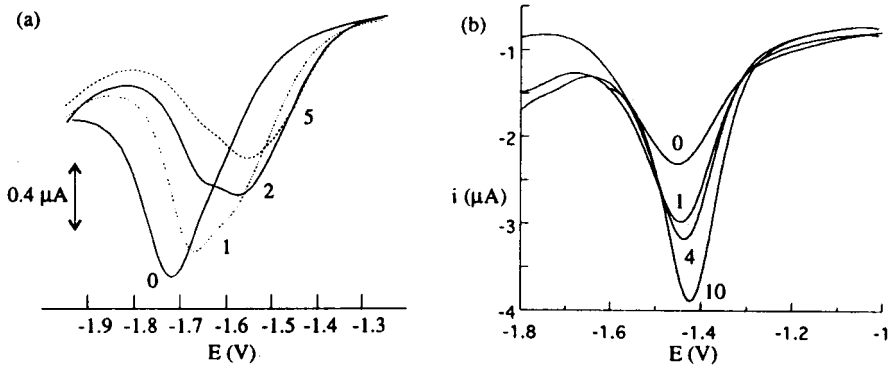

Figure 2. Changes in E_p upon addition of Ba^{2+} ions for the reduction of (a) compound **I** (prepared in situ) and (b) compound **V**, followed by DPV; numbers correspond to the amount of metal ion added (mol. equiv.)

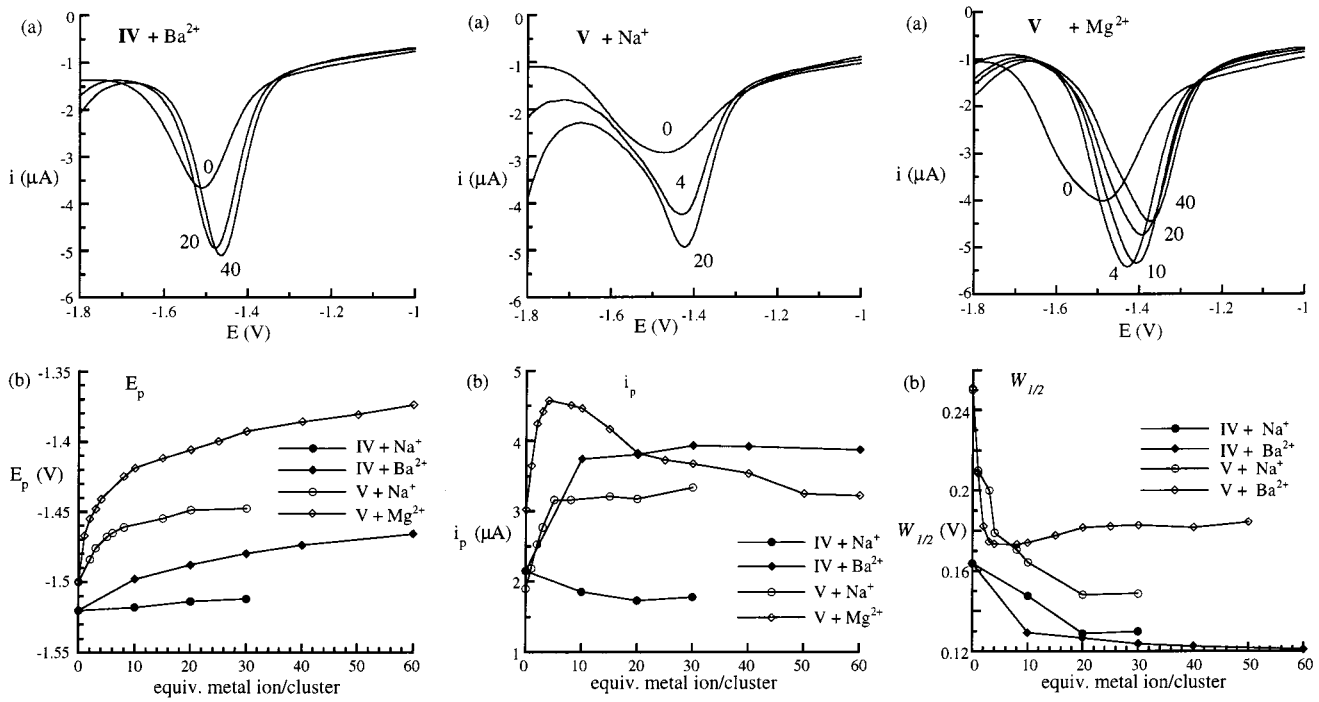

Figure 3. (a) DPV titrations of compound **IV** with Ba^{2+} ions, and compound **V** with Na^+ and Mg^{2+} ions, numbers correspond to the amount of metal ion added; (b) corresponding titration curves (including those for compound **IV** and Na^+) in which E_p, i_p, and $W_{1/2}$ are plotted as a function of the amount of metal ion added

modulator as well. Promoter/modulator effects similar to those observed for proteins have also been observed for semi-encapsulated, synthetic cluster compounds.[20][21]

Overlays of subsequent differential pulse voltammograms in the titration of cluster compounds **IV** with Ba^{2+} ions, and **V** with Na^+ and Mg^{2+} ions are shown in Figure 3a. Figure 3b shows the titration curves in which i_p, and $W_{1/2}$ (and also E_p, see below) are plotted as a function of the amount of metal ion added per cluster. The curves derived from the titration of **IV** with Na^+ ions are also shown. For compound **IV**, a small decrease in current response (i_p) was observed upon the addition of monovalent alkali metal ions. The addition of divalent metal ions clearly resulted in an increase in i_p as well as in the electrochemical reversibility of the redox process (decreased $W_{1/2}$ value). The i_p and $W_{1/2}$ values of **V** improved considerably upon the addition of monovalent as well as divalent metal ions, except in the case of Li^+ for which only minor improvements were observed (not shown).

The fact that divalent metal ions have an influence on the electrochemical properties of **IV** indicates that the overall negative charge of **IV** to some extent hampers a clean redox process. Divalent metal ions are assumed to form a layer of positive charges on a negatively charged electrode, thereby facilitating the reduction of negatively charged species, while monovalent metal ions do not give this effect.[22] This phenomenon can be explained by the larger polarizing strength of the divalent alkaline earth metal ions as compared to the monovalent alkali metal ions.

The addition of metal ions to cluster compound **V**, with the exception of Li^+, resulted in an improvement of the current response and in smaller $W_{1/2}$ values (vide supra). The titration curves in Figure 3b indicate that changes in these parameters are directly related to the amount of metal ion that is added to **V**. These promotion effects were already observed upon addition of less than four equivalents of metal ions per cluster. Binding of more than two monovalent metal ions by **V** converts this compound from an overall negatively to an overall positively charged species, resulting in a more favourable interaction with the negatively charged electrode. This observation is in sharp contrast to the large excess of $Ba(ClO_4)_2$ which is required to promote the electrochemistry of metalloproteins and the earlier mentioned semi-encapsulated cluster compounds.[19–21] This strongly suggests that specific binding of metal ions in the crown ether rings causes the observed effects. In addition, compound **IV**, having no specific metal ion binding sites, was only affected at metal ion concentrations approaching the millimolar range.

The promoter effects observed for cluster compound **I** were in line with those obtained for **V**, albeit less pronounced (not shown). Apparently, the larger flexibility of the crown ether ligands in **I** as compared to **V** results in a better electrochemical behaviour even without the addition of metal ions.

Changes in the peak potentials of compounds **IV** and **V** vary from 0 for Li^+ to 70 mV for Mg^{2+} after the addition of 10 equivalents of these ions per cluster compound (Table 3). In general, the changes of the E_p of **IV** are very small; a maximum modulation of 20–30 mV for divalent metal ions is observed. This small change may be the result of a weak coordination of the metal ions to the amide function

in the ligand, or may be caused by changes in the electrode surface as pointed out above. At very high metal ion concentration, larger effects were observed with Mg^{2+} and Ba^{2+}, suggesting that either of the two factors became more important in the modulation process.

For compound **V**, the modulation effects are more pronounced than for **IV**. The titration curves in Figure 3b show that the largest effect is achieved after the addition of several equivalents of Na^+. For Ba^{2+}, the major effect is achieved after the addition of approximately 20 equivalents (not shown). After the addition of an excess of modulator, minor additional changes in E_p were observed. These additional changes closely match the effects found for compound **IV** at low modulator concentrations.

In Figure 2a, an overlay of sequential voltammograms for the titration of compound **I** with Ba^{2+} is depicted (vide supra). Figure 4 presents the changes in E_p for this compound upon the addition of Ba^{2+}, Na^+, and K^+ ions. Due to the multi-wave behaviour observed in the Ba^{2+} titration and problems with the deconvolution, the Ba^{2+} curve in Figure 4 deviates from an ideal titration curve. Nevertheless it can be concluded that the effect of Ba^{2+} ions is much larger than the effects of K^+ and Na^+ ions. The addition of very small amounts of both Ba^{2+} and K^+ results in a steep rise in E_p, whereas for Na^+ this is not observed. In accordance with the observations for compound **V**, it is likely that the binding of ions in the crown ether ligands of the cluster contributes most to the observed changes in E_p. The fact that multi-wave behaviour is observed with Ba^{2+}, as well as with Li^+ and Mg^{2+} ions, points to a strong binding of these metal ions by compound **I**.

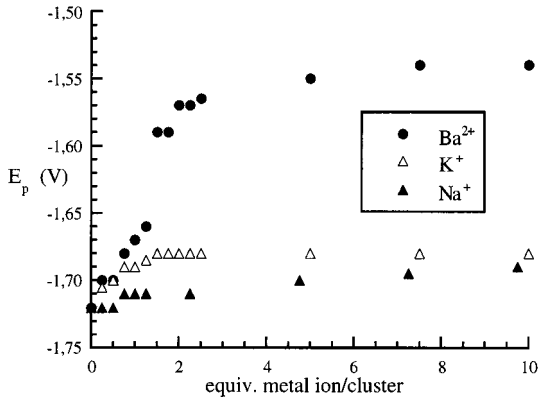

Figure 4. Changes in E_p upon titration of compound **I** with Na^+, K^+, and Ba^{2+} ions

Rationalization of the Modulator Effects

The different changes in E_p upon the addition of stoichiometric amounts of metal ions to cluster compounds **I** and **V** probably arise from the fact that the affinities of the crown ether ligands of the host compounds for the metal ions are different. As was mentioned in the introduction, the binding of metal ions in the monoaza-18-crown-6 ligands of **I** is expected to follow the trend $Li^+ \approx Mg^{2+} < Na^+ < K^+ \approx Ba^{2+}$, which is based on size complementarity. From the point of view of charge stabilization, the divalent metal ions are expected to bind more strongly than the monovalent metal ions.[6] The binding constants for the ligands of **V** were anticipated to be lower than those of the ligands of **I**. The acyl functions on the nitrogen centers in the aza crown ether rings of **V** lead to a host molecule which is a less efficient metal ion binder. This modification could explain the generally smaller changes in E_p found for **V**. However, these rules of thumb do not explain the trends in responses of compounds **I** and **V**.

Figure 5 shows the dependence of the modulation of the E_p of compound **I** on the charge density of the metal ion that causes the modulation. Metal ions bearing a high charge density give rise to a larger change in the reduction potential than metal ions bearing a low charge density. In other words, the higher the polarizing strength of the metal ion, the larger the modulation of the redox properties of the polarizable Fe_4S_4 core in **I**. It is likely therefore that this modulation is governed by electrostatic forces. In this way, metal ions with similar binding constants or ionic radii such as K^+ and Ba^{2+}, but different polarizing effects, bring about different modulations. Similar observations have been made by Hall et al. for their ferrocene based cryptates.[23]

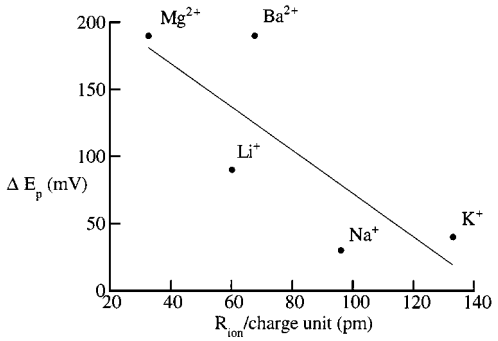

Figure 5. Dependence of the metal ion induced change in $E_{p,red}$ of compound **I** on the charge density of the metal ion

The multi-wave behaviour that is observed for **I** in combination with Ba^{2+}, Li^+, and Mg^{2+} ions, and the magnitude of the modulations, suggests that the binding of these metal ions by **I** is strong. Since the connection between the binding site and redox site in **I** is not conducting, the metal ions should be bound in very close proximity to the redox active center in order to be able to affect the redox potential to the observed extent. It is proposed therefore, that compound **I** binds metal ions in a lariat-ether fashion,[24] with the oxygen and nitrogen atoms of the crown ether ring and the negatively charged thiolate sulfur atom, which coordinates to the cluster, as donor atoms (see Figure 6). In this way the interaction between the binding site and the redox site would be through-bond instead of through-space and the overall negative charge of the cluster compounds would contribute to its interaction with metal ions. Similar lariat

interactions have been proposed before by Gokel et al. in nitrobenzene pivoted crown ethers.[25]

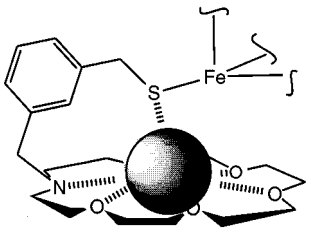

Figure 6. Proposed mode of metal ion binding by compound **I**

Due to conformational restrictions, the host-guest interaction in **V** is not expected to be similar to that of **I**. As in cluster compound **I**, there is no conducting connection between the redox center and the binding site in this compound. An effective impact on the redox potential of the cluster core should, therefore, arise via through-space interactions. The more rigid ligand connection in **V** compared to **I** is likely to result in a less favourable approach of the metal ion to the redox active center, which could explain that, in general, smaller modulation effects and no multiwave behaviour were observed for compound **V**. Combining the values from Table 3 with the curves in Figure 3b, and taking into account the metal ion charge densities, one can conclude that the binding constants in **V** roughly follow the trend $Li^+ < Ba^{2+} < Mg^{2+} < Na^+ < K^+$. In particular, acylation of the aza crown ether rings seems to influence the binding of metal ions with a high charge density in a negative sense. The modulation effects observed for **V** can then be explained by combining the known trend in binding constants with the polarizing strength of the metal ions.

Another way of dealing with the observed modulation effects is presented in Scheme 5, which is taken from earlier papers by Kaifer et al.[26] Starting from a redox-active host compound (an Fe_4S_4 cluster in this case) and an uncomplexed guest, there are two ways to come to a reduced host-guest complex. In one way, the guest is bound by the host compound in the first step, resulting in a facilitated reduction of the redox active center. In the second way, the redox-active center is first reduced, which in turn results in an enhanced binding of the guest.

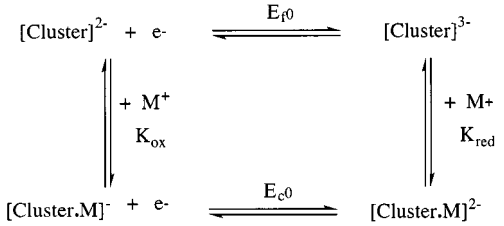

Scheme 5. Pathways for metal ion complexation in an Fe_4S_4 cluster compound; E_c^0 and E_f^0 are the midpoint potentials for the complex and the free ligand, respectively

For the respective reduction potentials and binding constants Equation 1 can be derived.[26]

$$E_p^{complex} - E_p^{free} = - RT/nF \, [\ln K_{red}/K_{ox}] \quad (1)$$

In words, the ratio of the binding constants of a guest in the reduced and oxidized host is given by the change in E_p brought about by the binding of the guest. In this model, the modulations that are observed for the cluster compounds reflect the enhanced binding of metal ions by these compounds upon reduction of the cluster core. Comparison of the modulations brought about by the different metal ions will then involve more than just the comparison of binding constants of the oxidized host. Equation 1 has been shown by Kaifer to be valid for systems with $K_{ox} > 10^4$. For systems with $1 < K_{ox} < 10^4$, which is expected to be the range for our compounds, the increase in binding constant is underestimated by this Equation.[26] The results of application of the above-mentioned analysis to the effects found for **I** and **V** are presented in Table 4.

Table 4. Ratio of K_{red} and K_{ox} for binding of different metal ions in compounds **I** and **V**[a]

	I	**V**
Li^+	33 (13)	–
Na^+	3 (1)	7 (3)
K^+	5 (2)	7 (3)
Mg^{2+}	1600 (650)	5 (2)
Ba^{2+}	1600 (650)	2 (1)

[a] Determined after the addition of 4 equivalents of metal ion. Estimated errors are given in parenthesis.

The titration curves presented in Figure 4 indicate that more than 2 and possibly 4 metal ions are bound to the crown ether cluster compounds. From our experiments it could not be determined whether the four binding sites behaved independently from each other, in terms of equal binding constants for every site, or that these sites influenced each other, e.g. by diminishing the binding of every next metal ion. It should be noted that applying Equation 1 might lead to overestimated values in the latter case. The numbers in Table 4 should therefore not be treated as absolute values but merely as representing trends in metal ion affinities of the cluster compounds.

Conclusion

A number of new thiolate-functionalized iron-sulfur cubane clusters **I**–**V** were prepared and characterized. In **I**, **III**, and **V**, the cluster cores are appended with binding sites for metal ions, viz. crown ether ligands. Electrochemical studies show that the large crown ether ligands hamper, to some extent, the electrochemical analysis of the cluster compounds. Only in the case of cluster compound **III** does the presence of the relatively large ligands have a pronounced effect on the $E_{1/2}$ value. Here, the ligands are believed to have a restricted conformational freedom, resulting in a more effective shielding of the cluster core.

Examination of the promotion and modulation effects of metal ions on cluster compounds **I**, **IV**, and **V** reveals that

the largest effects occur in the case of the crown ether functionalized cluster compounds **I** and **V**. Addition of stoichiometric amounts of metal ions leads to large changes in the electrochemical characteristics of the cluster reduction, implying that metal ions are bound in the crown ether ligands. Smaller changes arise from electrode modification, which facilitates the reduction of the negatively charged cluster compounds, as was shown for compound **IV**. Reduction of the cluster compounds enhances their affinity for alkali and alkaline earth metal ions. A lariat-binding mode is proposed for the complexation of metal ions to compound **I**, resulting in a more or less through-bond interaction between the redox site and the crown ether bound metal ion. In this way, binding of metal ions by this compound is favoured by the negative charge of its redox center. Such a favourable interaction was ruled out, however, for compound **V** due to restrictions in the conformation of its ligands; probably related to the lack of rotational freedom of the amide bonds. The modulations observed for compound **V** seem to take place via through-space interactions. Overall, the characteristic features of the modulations measured for the novel cluster compounds were shown to be governed by the interplay of crown ether selectivity, ligand flexibility, and electrostatic forces. As a result, the modulations observed for compounds **I** and **V** are in sharp contrast to each other. Whereas **I** shows a strong response towards Ba^{2+} ions and hardly any response towards K^+, compound **V** displays much smaller effects and an opposite selectivity.

The results presented here show that crown ether-functionalized iron-sulfur clusters can serve as electrochemically active host compounds, and can in principle be applied as building blocks for the construction of electrochemical sensory devices which are able to display selective responses towards charged species

Experimental Section

General Procedures: All chemicals were commercial products and were used as received. α-Chloroacetyl chloride was synthesized using a literature procedure.[27] Di-*n*-butylamine and thioacetic acid were distilled under reduced pressure. Diethyl ether was distilled from sodium metal/benzophenone, hexane was distilled from sodium metal, and dichloromethane and chloroform were distilled from $CaCl_2$. Pyridine and triethylamine were distilled from CaH_2. DMF used for electrochemical experiments was stored over BaO for at least one day, after which it was distilled under reduced pressure. Ethyl acetate used for flash chromatography was distilled from K_2CO_3/Na_2CO_3. Hexane used for the same purpose was distilled once using a rotary evaporator. All other solvents were used as received. Manipulations involving thiol compounds were performed under N_2 unless stated otherwise. Glassware used in thiol handling was left overnight in a hypochlorite solution to prevent stench. Manipulations involving iron-sulfur clusters were performed using standard Schlenk techniques. − Flash chromatography was performed on Silica Gel (60 H) purchased from Merck, or on neutral alumina purchased from Across. Prior to use, neutral alumina was activated to activity III, according to the Brockman scale.[28] − TLC analyses were performed on silica 60 F_{254} coated glass plates from Merck. Thiol compounds were detected by treatment of the TLC plates with a nitroprusside reagent.[29] − FT-IR spectra were recorded with a BioRad FTS 25 instrument. − UV/Vis spectra were recorded with a Perkin−Elmer Lambda 5 instrument. − ^{1}H-NMR spectra were recorded with Bruker WF-90, Bruker AC-100, Bruker WM-200, Bruker AC-300, or Bruker AM-400 instruments (internal standards: $CDCl_3$ as solvent TMS, δ_H = 0.00; [D_6]DMSO as solvent, δ_H = 2.50; [D_7]DMF as solvent, δ_H = 2.94). − Mass spectra were obtained from a VG 7070E instrument [FAB$^+$ (3-nitrobenzyl alcohol), EI$^+$]. − Elemental analyses were performed with a Carlo Erba EA 1180 instrument. − Melting points were measured with a Reichert−Jung Hotstage 600 instrument (uncorrected values). − Electrochemical analysis (CV, DPV) were performed with an EG & G Princeton Applied Research Model 273 Electrochemistry System equipped with Model 270 Electrochemical Analysis Software 200. Reference electrodes: Ag/AgCl (0.1 M LiCl) in DMF, Ag/AgI (0.02 M Bu_4NI/0.1 M Bu_4NPF_6) in CH_2Cl_2, and Ag/Ag$^+$ (0.1 M $AgNO_3$) in CH_3CN. Supporting electrolyte: 0.1 M tetrabutylammonium hexafluorophosphate (TBAH). All measurements were performed under an inert gas, using a conventional three-electrode electrochemical cell equipped with either platinum or PGE working and Pt auxiliary electrodes. PGE electrodes were polished with 0.3 μm alumina, rinsed with water, and sonicated in water for 10 min before use. Before every session, the experimental setup was tested using ferrocene and $[Fe_4S_4(S\mathit{t}Bu)_4](NBu_4)_2$. Halfwave and peak potentials are given against the reversible Fc/Fc$^+$ couple. Scan rates were 100 mV/s (CV) and 10 mV/s (DPV) unless stated otherwise. Concentrations of electroactive species were between 0.01 mM and 1 mM.

α-Bromo-α′-thioacetyl-*m*-xylene (1): To a solution of K_2CO_3 (1.05 g, 7.6 mmol) in 4 mL of DMF was slowly added a solution of freshly distilled thioacetic acid (1.14 g, 15 mmol) in 2 mL of DMF. After CO_2 formation had ceased, the resulting yellow solution was diluted with the same amount of DMF. This diluted solution was added dropwise to a solution of α,α′-dibromo-*m*-xylene (4.0 g, 15.2 mmol) in 20 mL of DMF, and the resulting mixture was stirred overnight under the exclusion of light. These manipulations were all performed under N_2. After filtration and removal of the solvent in vacuo, the resulting residue was dissolved in 100 mL of diethyl ether, washed with water (3×), dried with $MgSO_4$, filtered, and concentrated in vacuo. Purification by flash chromatography (silica, ethyl acetate/hexane = 1:10, v/v) yielded 2.1 g (54%) of **1** as a yellow oil. − ^{1}H NMR (90 MHz, $CDCl_3$): δ = 2.36 [s, 3 H, C(O)CH_2], 4.11 (s, 2 H, ArCH_2S), 4.45 (s, 2 H, ArCH_2Br), 7.29 (m, 4 H, Ar*H*). − EI-MS; *m*/*z*: 260 [M]$^+$. − $C_{10}H_{11}BrOS$ (259.2): calcd. C 46.35, H 4.28, S 12.37; found C 46.50, H 4.39, S 11.85.

1-(α-Thioacetyl-*m*-xylyl)-4,7,10,13,16-pentaoxa-1-azacyclooctadecane (2): A solution of **1** (390 mg, 1.51 mmol) in 5 mL of DMF was added dropwise to a solution of 4,7,10,13,16-pentaoxa-1-azacyclooctadecane (400 mg, 1.51 mmol) in 15 mL of DMF which contained some K_2CO_3 as a base. The reaction mixture was stirred overnight at 40°C under N_2, after which the solvent was removed under reduced pressure. The resulting oil was dissolved in 40 mL of dichloromethane, washed twice with a saturated aqueous $NaHCO_3$ solution, dried with $MgSO_4$, filtered, and concentrated in vacuo. Purification by flash chromatography (silica, $CHCl_3$/MeOH/TEA = 97:2:1, v/v) yielded 530 mg (80%) of **2** as a viscous yellow oil. − ^{1}H NMR (90 MHz, $CDCl_3$): δ = 2.36 [s, 3 H, C(O)CH_3], 2.78 (t, *J* = 6.6 Hz, 4 H, N$CH_2$$CH_2$O), 3.62 (m, 22 H, O$CH_2$, Ar$CH_2$N), 4.11 (s, 2 H, Ar$CH_2$S), 7.24 (m, 4 H, Ar*H*). − FAB-MS; *m*/*z*: 442 [M + 1]$^+$. − $C_{22}H_{35}NO_6S$ (441.6): C 59.84, H 7.99, N 3.17, S 7.26; found C 59.63, H 8.05, N 3.22, S 7.36.

1-(α-Mercapto-*m*-xylyl)-4,7,10,13,16-pentaoxa-1-azacyclooctadecane (L^{1}H): A solution of **2** (200 mg, 0.45 mmol) in 5 mL of 3%

HCl in methanol was stirred at ambient temperature for 3 d. At this point, TLC analysis showed one spot that was positive in a sodium nitroprusside test. To the reaction mixture were then added 20 mL of dichloromethane and 10 mL of water. The layers were neutralized using a saturated aqueous $NaHCO_3$ solution, after which the organic layer was washed once again with water. After drying with $MgSO_4$, filtration, and removal of the solvent under reduced pressure, 170 mg (95%) of **L^{1}H** was obtained as a yellowish oil. − ^{1}H NMR (90 MHz, $CDCl_3$): δ = 1.75 (t, *J* = 7.3 Hz, 1 H, *SH*), 2.78 (t, *J* = 6.0 Hz, 4 H, N*CH*$_2$CH$_2$O), 3.62 (m, 22 H, O*CH*$_2$, Ar*CH*$_2$N, Ar*CH*$_2$S), 7.24 (m, 4 H, Ar*H*). − $C_{20}H_{33}NO_5S$ (399.5): calcd. C 60.28, H 8.09, N 3.51, S 8.09; found C 60.44, H 8.24, N 3.67, S, 8.18.

(α-Chloroacetyl)di-*n*-butylamine (3): To a solution of di-*n*-butylamine (1.06 g, 7.8 mmol) in CH_2Cl_2 (75 mL) which contained 1.1 mL of triethylamine as a base, was added dropwise a solution of α-chloroacetyl chloride (875 mg, 7.75 mmol) in 25 mL of CH_2Cl_2. The reaction mixture was stirred overnight at ambient temperature and subsequently washed (3×) with a saturated aqueous $NaHCO_3$ solution, and dried with $MgSO_4$. Flash chromatography (silica, $CHCl_3$/MeOH = 98.5:1.5, v/v) gave **3** as a colourless oil in 26% yield. − ^{1}H NMR (90 MHz, $CDCl_3$): δ = 0.82−1.04 (m, 6 H, *CH*$_3$), 1.14−1.70 (m, 8 H, *CH*$_2$*CH*$_2$CH$_3$), 3.20−3.43 (m, 4 H, N*CH*$_2$), 4.07 (s, 2 H, *CH*$_2$Cl). − EI-MS; *m*/*z*: 205 $[M]^+$. − $C_{10}H_{20}ClNO$ (205.7): calcd. C 58.38, H 9.80, N 6.81; found C 57.95, H 10.17, N 6.87.

[α-(Thioacetyl)acetyl]di-*n*-butylamine (4): Under N_2, 299 mg (2.15 mmol) of K_2CO_3 was allowed to react with 155 μL of thioacetic acid in a minimum amount of DMF. The resulting solution was added dropwise to a solution of **3** (446 mg, 2.16 mmol) in DMF, and this mixture was stirred overnight under the exclusion of light. After removal of the solvent under reduced pressure, the residue was dissolved in CH_2Cl_2 and washed twice with brine and once with water. The organic layer was dried with $MgSO_4$. Flash chromatography (silica, $CHCl_3$/MeOH = 99:1, v/v) yielded **4** as a yellow oil in 65% yield (345 mg). − ^{1}H NMR (90 MHz, $CDCl_3$): δ = 0.84−1.05 (m, 6 H, CH$_2$CH$_2$*CH*$_3$), 1.19−1.73 (m, 8 H, *CH*$_2$*CH*$_2$CH$_3$), 2.39 [s, 3 H, C(O)*CH*$_3$], 3.22−3.43 (m, 4 H, N*CH*$_2$), 4.37 (s, 2 H, *CH*$_2$S). − FT-IR (KBr, cm^{-1}): $\tilde{\nu}$ = 2959, 2932, 2874 (CH_2, CH_3), 1695 (C=OCH$_3$), 1647 (C=O), 1428, 1377 (CH_2, CH_3), 1355 (C=OCH$_3$), 733 (CH_2). − EI-MS; *m*/*z*: 245 $[M]^+$. − $C_{12}H_{23}NO_2S$·0.5MeOH (260.4): calcd. C 57.44, H 9.64, N 5.36, S 12.26; found C 57.46, H 9.49, N 5.68, S 12.07.

(α-Mercaptoacetyl)di-*n*-butylamine (L^{2}H): To a solution of **4** (130 mg, 0.53 mmol) in 3 mL of CH_2Cl_2 was added 3 mL of 6% HCl in MeOH. The resulting mixture was stirred overnight. At this point, TLC analysis revealed a single spot that turned red when treated with nitroprusside. The reaction mixture was diluted with CH_2Cl_2 and neutralized with saturated aqueous $NaHCO_3$, washed once with water and dried with $MgSO_4$. Removal of the solvent in vacuo yielded 108 mg (100%) of **L^{2}H** as a brownish-yellow oil. − ^{1}H NMR (200 MHz, $CDCl_3$): δ = 0.99−0.89 (m, 6 H, CH$_2$CH$_2$*CH*$_3$), 1.26−1.37 (m, 4 H, CH$_2$*CH*$_2$CH$_3$), 1.49−1.61 (m, 4 H, *CH*$_2$CH$_2$CH$_3$), 2.17 (t, *J* = 7.43 Hz, 1 H, *SH*), 3.20−3.36 (m, 6 H, N*CH*$_2$CH$_2$, CH$_2$S). − FT-IR (KBr, cm^{-1}): $\tilde{\nu}$ = 2958−2863 (CH_2, CH_3), 2554 (SH), 1642 (C=O), 1454, 1430, 1376 (CH_2, CH_2). − EI-MS; *m*/*z*: 203 $[M]^+$. − No reproducible analysis could be obtained for this compound.

1-(α−Chloroacetyl)-4,7,10,13,16-pentaoxa-1-azacyclooctadecane (5): To a solution of 4,7,10,13,16-pentaoxa-1-azacyclooctadecane (300 mg, 1.14 mmol) in 15 mL of toluene, containing some solid K_2CO_3 as a base, a solution of α-chloroacetyl chloride (150 mg, 1.3 mmol) in 2 mL of toluene was added dropwise. The reaction mixture was stirred overnight at ambient temperature, after which the solvent was removed in vacuo. The resulting residue was dissolved in 50 mL of dichloromethane; this solution was washed twice with a saturated aqueous $NaHCO_3$ solution, dried with $MgSO_4$, and filtered. After removal of the solvent under reduced pressure, 350 mg (90%) of **5** was obtained. − ^{1}H NMR (90 MHz, $CDCl_3$): δ = 3.82 (m, 24 H, O*CH*$_2$, N*CH*$_2$), 4.24 (s, 2 H, *CH*$_2$Cl). − FT-IR (KBr, cm^{-1}): $\tilde{\nu}$ = 3003, 2872 (br, CH_2), 1648 (C=O), 1455, 1353 (CH_2), 1121 (COC), 712 (CH_2). − EI-MS; *m*/*z*: 340 $[M]^+$. − $C_{14}H_{26}ClNO_6$ (339.8): calcd. C 49.54, H 7.73, N 4.13; found C 49.45, H 7.84, N 4.09.

1-[α-(Thioacetyl)acetyl]-4,7,10,13,16-pentaoxa-1-azacyclooctadecane (6): To prepare this compound, a similar procedure as described for the synthesis of **4** was used. A DMF solution of potassium thioacetate, prepared from K_2CO_3 (100 mg, 0.72 mmol) and thioacetic acid (100 mg, 1.3 mmol), was added to a DMF solution containing **5** (350 mg, 1.03 mmol). After workup using dichloromethane and flash chromatography (silica, $CHCl_3$/MeOH = 98:2, v/v) compound **6** (250 mg, 61%) was obtained as a viscous, yellow oil. − ^{1}H NMR (300 MHz, $CDCl_3$): δ = 2.38 (s, 3H, *CH*$_3$), 3.50−3.81 (m, 24 H, O*CH*$_2$, N*CH*$_2$), 3.98 (s, 2 H, *CH*$_2$S). − ^{13}C NMR (75 MHz, $CDCl_3$): δ = 30.5 (CH_3), 32.5 (SCH_2), 48.0 (NCH_2), 70.0−71.5 (m, OCH_2), 168.5 (NC=O), 196.0 (SC=O). − FT-IR (KBr, cm^{-1}): $\tilde{\nu}$ = 2867 (br, CH_2, CH_3), 1691 (SC=O), 1656, 1648 (C=O), 1468, 1450 (CH_2, CH_3), 1353 ($COCH_3$), 1120 (COC), 732 (CH_2). − EI-MS; *m*/*z*: 379 $[M]^+$. − No reproducible analysis could be obtained for this compound.

1-(α-Mercaptoacetyl)-4,7,10,13,16-pentaoxa-1-azacyclooctadecane (L^{3}H): This compound was prepared using the procedure described for compound **L^{2}H**. Starting from **6** (100 mg, 0.24 mmol), 77 mg (95%) of ligand **L^{3}H** was isolated. − ^{1}H NMR (300 MHz, $CDCl_3$): δ = 2.17 (t, *J* = 7.52 Hz, 1 H, *SH*), 3.40−3.76 (m, 26 H, O*CH*$_2$, N*CH*$_2$, S*CH*$_2$). − ^{13}C NMR (75 MHz, $CDCl_3$): δ = 27.0 ($HSCH_2$), 47.83 (NCH_2), 70.03−71.78 (m, OCH_2), 171.1 (NC=O). − FT-IR (KBr, cm^{-1}): $\tilde{\nu}$ = 2867 (br, CH_2), 2546 (SH), 1654 (C=O), 1448, 1421 (CH_2), 1119 (br, COC). − EI-MS; *m*/*z*: 338 $[M]^+$. − No reproducible analysis could be obtained for this compound.

2,2′-Dithiobisbenzoic Acid (7):[30] To a solution of thiosalicylic acid (8 g, 51.9 mmol) and NaOH (6.4 g, 160 mmol) in 60 mL of water was added very slowly, by means of a dropping funnel, 25 mL of a solution of 15% H_2O_2 in water. During the addition the reaction mixture was cooled on ice. After the addition was completed the mixture was slowly allowed to come to ambient temperature. Finally, it was stirred overnight at 60°C. The mixture was again cooled on ice, and neutralized with aqueous 2N HCl, which resulted in the formation of a white precipitate. The product was filtered off, washed with cold ethanol and cold water, and dried in vacuo. This procedure yielded 6.3 g (80%) of **7** as a white powder, m.p. 298−299°C. − ^{1}H NMR (90 MHz, [D$_6$]DMSO): δ = 7.39 (m, 2 H, Ar*H*$^{4,4'}$), 7.62 (m, 4 H, Ar*H*$^{5,5'}$, Ar*H*$^{6,6'}$), 8.04 (m, 2H, Ar*H*$^{3,3'}$). − FT-IR (KBr, cm^{-1}): $\tilde{\nu}$ = 3500−2500 (OH), 1673 (C=O), 735 (ArH). − FAB-MS; *m*/*z*: 306 $[M]^+$. − $C_{14}H_{10}O_4S_2$·0.25EtOH (317.8): calcd. C 56.20, H 3.74, S 20.69; found C 56.20, H 3.36, S 20.81.

***N*,*N*,*N*′,*N*′-Tetra-*n*-butyl-2,2′-dithiobisbenzoylamine (9):** A suspension of **7** (410 mg, 1.33 mmol) in 10 mL of $SOCl_2$ was heated under reflux overnight, yielding a clear solution. After removal of the excess of $SOCl_2$ in vacuo, the resulting residue, **8**, was dissolved in 5 mL of dichloromethane. This solution was then added dropwise to a solution of di-*n*-butylamine (387 mg, 3.0 mmol) and of triethylamine (220 μL) in 50 mL of dichloromethane. The reaction mixture

was stirred overnight at ambient temperature, after which it was washed (3×) with a saturated aqueous $NaHCO_3$ solution. The organic layer was dried with $MgSO_4$, filtered, and concentrated. After purification by flash chromatography (alumina, CH_2Cl_2/EtOH = 99:1, v/v) compound **9** (650 mg, 82%) was obtained as a yellowish, viscous oil. − ^{1}H NMR (90 MHz, $CDCl_3$): δ = 0.90 (m, 12 H, $CH_2CH_2CH_3$), 1.50 (m, 16 H, $CH_2CH_2CH_3$), 3.10 (t, *J* = 8.2 Hz, 4 H, NCH_2CH_2), 3.52 (t, *J* = 7.4 Hz, 4 H, NCH_2CH_2), 7.24 (m, 6 H, Ar*H*$^{4,4'}$, Ar*H*$^{5,5'}$, Ar*H*$^{6,6'}$), 7.67 (m, 2 H, Ar*H*$^{3,3'}$). − FAB-MS; *m*/*z*: 529 $[M + H]^+$. − No reproducible analysis could be obtained for this compound.

***N*,*N*-Di-*n*-butyl-2-mercaptobenzoylamine (L^4H):** A solution of **9** (528 mg, 1.0 mmol) and triphenylphosphane (263 mg, 1.0 mmol) in a mixture of aqueous 37% HCl (2.5 mL), water (7.5 mL), and dioxane (40 mL) was stirred overnight at 40 °C. The organic solvent was removed under reduced pressure and 100 mL of dichloromethane was added to the residue. The organic layer was washed (3×) with a saturated aqueous $NaHCO_3$ solution, dried with $MgSO_4$, filtered, and concentrated. Purification by means of flash chromatography (alumina, CH_2Cl_2/EtOH = 99:1, v/v) yielded 420 mg (80%) of L^4H as a viscous oil. − ^{1}H NMR (90 MHz, $CDCl_3$): δ = 0.90 (m, 6 H, $CH_2CH_2CH_3$), 1.50 (m, 8 H, $CH_2CH_2CH_3$), 3.10 (t, *J* = 8.0 Hz, 2 H, NCH_2CH_2), 3.52 (t, *J* = 8.0 Hz, 2 H, NCH_2CH_2), 4.74 (s, 1 H, *SH*), 7.25 (m, 4 H, Ar*H*). − FT-IR (KBr, cm^{-1}): $\tilde{\nu}$ = 3055 (Ar), 2958, 2932, 2872 (CH_2, CH_3), 2519 (SH), 1628 (C=O), 1462, 1425, 1377 (CH_2, CH_3), 773, 747 (ArH). − EI-MS; *m*/*z*: 265 $[M]^+$. − $C_{15}H_{23}NOS{\cdot}0.5EtOH$ (288.4): calcd. C 66.62, H 9.09, N 4.86, S 11.11; found C 66.71, H 8.64, N 5.31, S 11.01.

***N*,*N*′-(2,2′-Dithiobenzoyl)bis(4,7,10,13,16-pentaoxa-1-azacyclooctadecane) (10):** To prepare this compound, a similar procedure as described for **9** was used. Starting from 4,7,10,13,16-pentaoxa-1-azacyclooctadecane (395 mg, 1.5 mmol), 478 mg (80%) of **10** was obtained as a yellowish, viscous oil after flash chromatography (alumina, CH_2Cl_2/EtOH = 95:5, v/v). − ^{1}H NMR (90 MHz, $CDCl_3$): δ = 3.71 (m, 24 H, OCH_2, NCH_2), 7.39 (m, 2 H, Ar*H*$^{4,4'}$), 7.62 (m, 4 H, Ar*H*$^{5,5'}$, Ar*H*$^{6,6'}$), 8.04 (m, 2 H, Ar*H*$^{3,3'}$). − FAB-MS; *m*/*z*: 835 $[M + K]^+$, 819 $[M + Na]^+$, 797 $[M + H]^+$. − $C_{38}H_{56}N_2O_{12}S_2{\cdot}0.5EtOH$ (831.2): calcd. C 56.81, H 7.31, N 3.44, S 7.88; found C 57.14, H 7.04, N 3.71, S 7.55.

2-Mercaptobenzoyl-4,7,10,13,16-pentaoxa-1-azacyclooctadecane (L^5H): This compound was prepared in a similar way as ligand L^4H. Starting from **10** (200 mg, 0.25 mmol) and triphenylphosphane (66 mg, 0.25 mmol), compound L^5H was obtained in 75% yield (150 mg) after flash chromatography (alumina, CH_2Cl_2/EtOH = 95:5, v/v). − ^{1}H NMR (90 MHz, $CDCl_3$): δ = 3.50−3.63 (m, 24 H, OCH_2, NCH_2), 3.86 (s, 1 H, *SH*), 7.25 (m, 4 H, Ar*H*). − EI-MS; *m*/*z*: 399 $[M]^+$. − No reproducible analysis could be obtained for this compound.

Synthesis of Cluster Compounds: In situ synthesis of cluster compounds **I**−**V** for initial electrochemical characterization was performed by the stepwise addition of 4−6 equivalents of thiol ligand and 4−6 equivalents of base to the appropriate amount of $(PPh_4)_2[Fe_4S_4Cl_4]$ in DMF. A stock solution of 0.081 M of $[Bu_4N]OH$ in methanol was used as the base. Differential pulse voltammograms were recorded after the addition of each equivalent ligand and base, and after equilibration. Typically, 1.8 mg (1.54 μmol) of $(PPh_4)_4[Fe_4S_4Cl_4]$ was used in these experiments. Quantitative synthesis of the cluster compounds for detailed characterization was performed by using either the chloro cluster reaction starting from $(PPh_4)_2[Fe_4S_4Cl_4]$, or the ligand exchange reaction starting from $(Bu_4N)_2[Fe_4S_4(StBu)_4]$. The starting materials, $(PPh_4)_2[Fe_4S_4Cl_4]$[31] and $(Bu_4N)_2[Fe_4S_4(StBu)_4]$[32] were synthesized using published methods.

$(Bu_4N)_2[Fe_4S_4(L^1)_4]$ (I): To a stirred solution of $(PPh_4)_2[Fe_4S_4Cl_4]$ (38.2 mg, 0.033 mmol) in 15 mL of DMF was added a solution of L^1H (65 mg, 0.163 mmol, 5 equiv.) in 5 mL DMF. After this addition was completed, 2 mL of 0.081 M $[Bu_4N]OH$ in methanol was added dropwise to the reaction mixture. After stirring for several hours, the reaction mixture was filtered and then concentrated in vacuo, followed by the addition of Et_2O to induce precipitation of the desired product. Storage at −20 °C overnight resulted in the formation of the tetrabutylammonium salt **I**, which was isolated as a black oil after decanting the supernatant and drying in vacuo (yield not determined). − ^{1}H NMR (90 MHz, $[D_6]$DMSO): δ = 0.81−1.10 [m, br., 24 H, CH_3 (NBu_4)], 1.19−1.81 [m, br., 32 H, $CH_2CH_2CH_3$ (NBu_4)], 2.68 (NCH_2, the structure of this peak is obscured by the solvent peak), 3.02−3.36 [m, 16 H, NCH_2 (NBu_4)], 3.36−3.75 (m, 104 H, OCH_2, NCH_2, NCH_2Ar), 7.20 [m, br., 4 H, Ar*H*], 7.49−7.90 (m, 12 H, Ar*H*), 15.08 [ds, br, 8 H, SCH_2]. − UV/Vis (DMF): λ_{max} (nm) = 300 (sh), 420.

$(Bu_4N)_2[Fe_4S_4(L^2)_4]$ (II): To a solution of the thiol ligand L^2H (55 mg, 0.27 mmol) in 5 mL of DMF was added dropwise a solution/suspension of $(Bu_4N)_2[Fe_4S_4(StBu)_4]$ (54.6 mg, 0.056 mmol) in 10 mL of DMF. The resulting black solution was stirred for several hours under dynamic vacuum, and overnight under N_2. After filtration, the volume was reduced in vacuo to about 1 mL and a large amount of Et_2O was added. The Schlenk vessel was placed at −20 °C overnight, which resulted in the precipitation of a black powder. The product was finally isolated by decantation of the supernatant, washing with Et_2O, and drying under vacuum. This procedure gave **II** as a black oil in 91% yield (84 mg). − ^{1}H NMR (200 MHz, $[D_6]$DMSO): δ = 0.87−0.97 (m, 48 H, CH_3), 1.29−1.56 (m, 64 H, CH_2CH_3, NCH_2CH_2), 3.18−3.33 (m, 32 H, NCH_2), 13.83 [s, br, 8 H, SCH_2]. − UV/Vis (DMF): λ_{max} (nm) = 301, 415, 620 (sh).

$(Bu_4N)_2[Fe_4S_4(L^3)_4]$ (III): This compound was prepared using the procedure described for compound **II**. Starting from L^3H (98.4 mg, 0.29 mmol, 5 equiv.) and $(Bu_4N)_2[Fe_4S_4(StBu)_4]$ (69.6 mg, 0.058 mmol), a black oil was obtained. The yield was not determined. − ^{1}H NMR (200 MHz, $[D_7]$DMF): δ = 1.05 [s, br, 24 H, CH_3 (NBu_4)], 1.49 [s, br, 16 H, CH_2CH_3 (NBu_4)], 1.85 [s, br, 16 H, NCH_2CH_2 (NBu_4)], 3.40−4.13 [m, 112 H, OCH_2, NCH_2, NCH_2 (NBu_4)], 15.35, 16.58 [d, br, 8 H, SCH_2]. − UV/Vis (DMF): λ_{max} (nm) = 300, 410, 660 (sh).

$(Bu_4N)_2[Fe_4S_4(L^4)_4]$ (IV): This compound was prepared using the procedure described for compound **II**, using L^4H (18.5 mg, 0.7 mmol, 5.8 equiv.) and $(Bu_4N)_2[Fe_4S_4(StBu)_4]$ (14.3 mg, 0.12 mmol). THF was used as the nonsolvent in the isolation of the black oil, **IV** (yield was not determined). Inspection of the ^{1}H-NMR spectrum showed that this compound was contaminated with some free ligand L^4H. − ^{1}H NMR (200 MHz, $[D_6]$DMSO): δ = 0.64−1.57 (m, 112 H, $CH_2CH_2CH_3$), 2.95−3.45 [m, 32 H, NCH_2, NCH_2 (NBu_4)], 3.73 [s, br, 4 H, *p*Ar*H*], 5.32 [s, br., 4 H, *o*Ar*H*], 7.97 [s, br., 4 H, *m*Ar*H*], 8.28 [s, br, 4 H, *m*Ar*H*]. − UV/Vis (DMF): λ_{max} (nm) = 307 (sh), 458.

$(Bu_4N)_2[Fe_4S_4(L^5)_4]$ (V): This compound was prepared using the procedure described for compound **II**. Amounts used were: 32 mg (0.08 mmol, 6.3 equiv.) of L^5H and 15.18 mg (0.013 mmol) of $(Bu_4N)_2[Fe_4S_4(StBu)_4]$. The yield of the black oil, **V**, was not determined. − ^{1}H NMR (90 MHz, $[D_6]$DMSO): δ = 0.79−1.09 [m, 24 H, CH_3 (NBu_4)], 1.09−1.78 [m, 32 H, $CH_2CH_2CH_3$ (NBu_4)], 3.01−3.94 [m, 114 H, NCH_2, OCH_2, *p*Ar*H*, NCH_2 (NBu_4)], 5.29

[s, br, 4 H, *o*Ar*H*], 7.96 [s, br, 4 H, *m*Ar*H*], 8.39 [s, br, 4 H, *m*Ar*H*]. – UV/Vis (DMF): λ_{max} (nm) = 307 (sh), 452.

Acknowledgments

This work was supported by the Dutch Foundation for Chemical Research (SON) with financial aid from the Dutch Foundation for Scientific Research (NWO). The authors would like to thank Dr. J. G. M. van der Linden for fruitful discussions and Mrs. A. M. Roelofsen for help with electrochemical experiments. In addition, R. Fokkens of the Institute for Mass Spectrometry at the University of Amsterdam is acknowledged.

[1] [1a] R. Cammack, *Adv. Inorg. Chem.* **1992**, *38*, 281–322. – [1b] H. Beinert, R. H. Holm, E. Münck, *Science* **1997**, *277*, 653–659.
[2] Only recently was evidence provided for an all-ferrous Fe_4S_4 cluster in biology, viz. in the Fe protein of *Azotobacter vinelandii* nitrogenase. The structure of this cluster has not been determined yet. See: [2a] H. C. Angove, S. J. Yoo, B. K. Burgess, E. Münck, *J. Am. Chem. Soc.* **1997**, *119*, 8730–8731. – [2b] K. B. Musgrave, H. C. Angove, B. K. Burgess, B. Hedman, K. O. Hodgson, *J. Am. Chem. Soc.* **1998**, *120*, 5325–5326.
[3] R. H. Holm, S. Ciurli, J. A. Weigel, *Prog. Inorg. Chem.* **1990**, *38*, 1–74.
[4] J. M. Berg, R. H. Holm in *Iron Sulfur Clusters* (Ed.: T. G. Spiro), J. Wiley & Sons, New York, **1983**, pp. 1–66.
[5] P. D. Beer, *Adv. Inorg. Chem.* **1992**, *39*, 79–157.
[6] [6a] R. M. Izatt, K. Pawlak, J. S. Bradshaw, R. L. Bruening, *Chem. Rev.* **1991**, *91*, 1721–2085. – [6b] R. M. Izatt, J. S. Bradshaw, S. A. Nielsen, J. D. Lamb, J. J. Christensen, D. Sen, *Chem. Rev.* **1985**, *85*, 271–339.
[7] B. Strijtveen, R. M. Kellogg, *J. Org. Chem.* **1986**, *51*, 3664–3671.
[8] H. Okuno, K. Uoto, T. Tomohiro, Y. Youinou, *J. Chem. Soc., Dalton Trans.* **1990**, 3375–3381.
[9] L. Overman, S. Smoot, J. D. Overman, *Synthesis* **1974**, 59–60.
[10] L. Que, Jr., M. A. Bobrik, J. A. Ibers, R. H. Holm, *J. Am. Chem. Soc.* **1974**, *96*, 4168–4177.
[11] Kinetic studies on this type of exchange reaction have been performed by Henderson et al. They showed that in the absence of acid a thiolate ligand first dissociates from the cluster, leaving one iron center with a vacant coordination site, followed by nucleophilic attack at this center of a second thiolate. In the presence of acid, the dissociation of the first thiolate is facilitated by protonation. See: R. A. Henderson, K. E. Oglieve, *J. Chem. Soc., Dalton Trans.* **1993**, 1467–1472.
[12] B. V. DePamphilis, B. A. Averill, T. Herskovitz, L. Que, Jr., R. H. Holm, *J. Am. Chem. Soc.* **1974**, *96*, 4159–4167.
[13] See for example: S. Ciurli, M. Carrié, J. A. Weigel, M. J. Carney, T. D. P. Stack, G. C. Papaefthymiou, R. H. Holm, *J. Am. Chem. Soc.* **1990**, *112*, 2654–2664.
[14] R. H. Holm, W. D. Philips, B. A. Averill, J. J. Mayerle, T. Herskowitz *J. Am. Chem. Soc.* **1974**, *96*, 2109–2117.
[15] J. G. Reynolds, E. J. Laskowski, R. H. Holm, *J. Am. Chem. Soc.* **1978**, *100*, 5315–5322.
[16] See for example: I. Bertini, F. Briganti, C. Luchinat, A. Scozzafava, M. Sola, *J. Am. Chem. Soc.* **1991**, *113*, 1237–1245.
[17] See: A. Nakamura, N. Ueyama, *Adv. Inorg. Chem.* **1989**, *33*, 39–67, and references cited therein.
[18] H. L. Blonk, Ph. D. Dissertation, Univ. of Nijmegen, **1991**.
[19] [19a] A. M. Bond, H. A. O. Hill in *Metal Ions in Biological Systems*, vol. 27 (Ed.: H. Siegel, A. Siegel), Marcel Dekker, Inc., New York, **1991**, p. 432–494. – [19b] F. A. Armstrong, H. A. Heering, J. Hirst, *Chem. Soc. Rev.* **1997**, *26*, 169–179.
[20] [20a] C. F. Martens, M. M. G. Bongers, P. J. A. Kenis, R. Czajka, M. C. Feiters, J. G. M. van der Linden, R. J. M. Nolte, *Chem. Ber./Recueil* **1997**, *130*, 23–33. – [20b] C. F. Martens, H. L. Blonk, T. Bongers, J. G. M. van der Linden, G. Beurskens, P. T. Beurskens, J. M. M. Smits, R. J. M. Nolte, *J. Chem. Soc., Chem. Commun.* **1991**, 1623–1625.
[21] [21a] G. P. F. van Strijdonck, J. A. E. H. van Haare, P. J. M. Hönen, R. C. G. M. van der Schoor, M. C. Feiters, J. G. M. van der Linden, J. J. Steggerda, R. J. M. Nolte *J. Chem. Soc., Dalton Trans.* **1997**, 449–461. – [21b] G. P. F. van Strijdonck, J. A. E. H. van Haare, J. G. M. van der Linden, J. J. Steggerda, R. J. M. Nolte, *Inorg. Chem.* **1994**, *33*, 999–1000.
[22] F. A. Armstrong, P. A. Cox, H. A. O. Hill, V. J. Lowe, B. N. Oliver, *J. Electroanal. Chem.* **1987**, *217*, 331–366.
[23] C. D. Hall, N. W. Sharpe, I. P. Danks, Y. P. Sang, *J. Chem. Soc., Chem. Commun*. **1989**, 419–421.
[24] For a review on lariat ethers, see: G. W. Gokel, *Chem. Soc. Rev.* **1992**, 41–47.
[25] A. E. Kaifer, D. A. Gustowski, L. Echegoyen, V. J. Gatto, R. A. Schultz, T. P. Cleary, C. R. Morgan, D. M. Golli, A. M. Rios, G. W. Gokel, *J. Am. Chem. Soc.* **1985**, *107*, 1958–1965.
[26] S. R. Miller, D. A. Gustowski, Z. Chen, G. W. Gokel, L. Echegoyen, A. E. Kaifer, *Anal. Chem.* **1988**, *60*, 2021–2024.
[27] R. Adams, L. H. Ulich, *J. Am. Chem. Soc.* **1920**, *42*, 599–611.
[28] H. Brockman, H. Schodder, *Ber. Dtsch. Chem. Ges.* **1941**, *74B*, 73–78.
[29] G. Tonnies, J. J. Kolb, *Anal. Chem.* **1951**, *23*, 823–826.
[30] Although this compound is commercially available, its purity was not sufficient for our purposes.
[31] G. Christou, C. D. Garner, *J. Chem. Soc., Dalton Trans.* **1979**, 1093–1094.
[32] G. B. Wong, M. A. Bobrik, R. H. Holm, *Inorg. Chem.* **1978**, *17*, 578–584.

Received March 11, 1999
[I99094]